PHYSICAL REVIEW A

GENERAL PHYSICS

THIRD SERIES, VOLUME 38, NUMBER 3 AUGUST 1, 1988

Electronic structure of the Fe_2 molecule in the local-spin-density approximation

S. Dhar and N. R. Kestner

Department of Chemistry, Louisiana State University, Baton Rouge, Louisiana 70803

(Received 15 June 1987; revised manuscript received 21 March 1988)

Ab initio self-consistent all-electron spin-polarized calculations have been performed for the ground-state properties of the Fe_2 molecule using the local-spin-density approximation. A Gaussian orbital basis is employed and all the two-electron integrals are evaluated analytically. The matrix elements of the exchange-correlation potential are computed numerically. The total energy, the binding energy, the equilibrium distance, vibrational frequency, and the ground-state configurations are reported and compared with other calculations and experimental results.

I. INTRODUCTION

During the past few years a great deal of effort has been devoted to experimental and theoretical investigations striving to understand the electronic structure of small transition-metal clusters, particularly diatomic molecules. These molecules are interesting both for themselves and for their relevance to surface science and heterogeneous catalysis. Therefore it is essential to acquire a profound insight into the electronic structure of these clusters at the atomic and molecular levels in order to calculate to elucidate their chemical and physical properties.

Both experimental and theoretical investigations of transition metal molecules are difficult to perform and are therefore dependent on one another for proper interpretations. For elements with partially filled d shells considerable complications arise in the theoretical investigation of the clusters because of the large number of possible configurations, which result from the degeneracy of the atomic d orbitals. Furthermore, the degree of uncertainty and complexity increases as the number of holes in the d shell increases, reaching a maximum when the d shell is half full.

Although a large number of experimental studies[1–14] have been carried out in the past few years, experimental problems with third-row transition-metal dimers—with the exception of the copper molecule (a full d-shell atom) cause spectroscopic data to be scarce and rather uncertain. High-temperature mass spectrometric methods[1–6] have been used for estimating the dissociation energies, but the dissociation energies so established depend on the values of the other spectroscopic constants assumed—such as equilibrium distance, vibrational frequency, and low-lying electronic states.

Experimentally, the internuclear separation is often approximated by the sum of the Pauling covalent single-bond radii, and the vibrational frequencies are interpolated using empirical formulas. However, the multiplicity and the symmetry of the electronic ground state of many of the dimers are still unknown. Recently Cox *et al.*[7] were able to determine the multiplicity and symmetry of the Fe_2 molecule for the state with highest angular momentum. This is a significant new piece of experimental data but it does not definitely establish the ground state.

Matrix isolation techniques[8–11] are also used for the transition-metal molecules. This forms the basis for other types of experimental investigations, such as Mössbauer and electron-spin-resonance (ESR) studies. From these data some of the ground-state molecular properties can be delineated by some semiempirical calculations. Gas-phase spectroscopic investigations of these molecules are still rather scarce, but increasing rapidly.[12–14]

Theoretical investigations of the ground-state configuration of the Fe_2 molecule have led to somewhat conflicting conclusions, depending on the method used. All of the *ab initio* Hartree–Fock (HF) calculations to data with few exceptions support low-spin states for diatomic transition-metal molecules, whereas calculations based on local-spin-density (LSD) approximations lead to high-spin ground states.

In HF calculations, the Fe_2 molecule is not bound; predictions are made about the ground-state configuration by analyzing Mössbauer data, but the conclusions arrived at are different depending on who does the analysis. Table I summarizes the spectroscopic data of the Fe_2 molecule, as obtained in various experiments and theoretical calculations.

The unrestricted Hartree Fock (UHF) procedure was used by Kelires *et al.*[15] for analysis of the Mössbauer

data. They used contracted Gaussian functions $9s,4p,3d$ with exponents and contraction coefficients given by Wachters.[16] Their study of quadrupole interaction and isomer shift supported the $^3\Sigma_g$ ground state for the Fe_2 molecule. Their calculations were performed only at two internuclear distances—3.78 and 3.53 a.u.

Semiempirical extended Hückel calculations of Copper, Clarke, and Hare[17] also suggest a $^3\Sigma_g$ state for the Fe_2 molecule. They performed the calculations with two sets of basis functions: (i) one that included $3p$, $3d$, and $4s$ functions, and (ii) one that included $3d$, $4s$, and $4p$ functions. The calculations with the first basis set resulted in a binding energy of 3.10 eV and an equilibrium distance of 3.59 a.u., while the corresponding values with the second set of functions were 5 eV and 2.36 a.u.

The extended Hückel studies of Mössbauer data followed by spin-polarized configuation interaction for valence electrons by Trautwein and Harris[18] predict an internuclear separation of 7.54 a.u. for the Fe_2 molecule.

The *ab initio* restricted Hartree Fock (RHF) calculations of Wolf and Schmidtke[19] suggested a $^1\Sigma_g$ ground state for the Fe_2 molecule with an equilibrium interatomic separation of 2.91 a.u. The only configuration interaction (CI) with single HF reference on Fe_2 is that due to Shim and co-workers.[4,20] They have performed CI calculations for 112-low-lying electronic states of Fe_2. They performed the calculations with two sets of basis functions: (i) Wachter's[16] basis set, which does not include a diffuse d function, and (ii) a basis set that included a diffuse d function. Their calculations suggest a $^7\Delta_u$ ground state. The large and small basis sets give binding energies of 0.04 and 0.69 eV, respectively, relative to the Fe atomic configuration of $3d^74s^1$. However, relative to Fe atoms in their ground state ($3d^64s^2$), their Fe_2 molecule is not bound. The calculations with large basis set resulted in an equilibrium distance of 4.99 a.u. and a vibrational frequency of 134 cm^{-1}, while the corresponding values with the smaller basis set are 4.54 a.u. and 204 cm^{-1}.

A few theoretical investigations of Fe_2 within the framework of density functional (DF) theory are also reported in the literature. Harris and Jones,[21] using a local-spin-density approximation, predicted the ground state of the Fe_2 molecule to be $^7\Delta_u$, with a binding energy of 3.45 eV, an equilibrium interatomic separation of 3.96 au., and a vibrational frequency of 390 cm^{-1}. However, their calculations are not fully spin-polarized and also use a pseudopotential with muffin-tin approximation.

Gvenzburger and Saitovitch[22] reported a discrete variational method (DVM), $X\alpha$ ($\alpha=\frac{2}{3}$) calculation, and used it to analyze the Mössbauer data at an interatomic separation of 3.53 a.u. The calculation is spin restricted and the most likely ground state predicted by them for Fe_2 is $^7\pi_u$.

Nagarathna *et al.*[23] have performed $X\alpha$-scattered-wave (SW) calculations on Fe_2. The α parameter for iron was taken as Schwarz's[24] value, which satisfied the virial theorem. The calculations included a muffin-tin-type approximation with overlapping spheres and their calculations were dependent on the degree of overlap of the Norman spheres.[25] However, they found that, for all overlaps of the Norman spheres, $^7\Delta_u$ had the lowest relative energy with an internuclear separation of 3.78 a.u., but the binding energy was not reported. Nevertheless, their investigations of the Mössbauer data suggested a $^7\Sigma_g$ or $^9\Sigma_g$ as the most probable ground state with an interatom-

TABLE I. Spectroscopic data of the Fe_2 molecule, as obtained in various experiments and theoretical calculations.

Method	State	Spectroscopic constant: Equilibrium distance r_e (a.u.)	Spectroscopic constant: Vibrational frequency ω (cm^{-1})	Binding energy D_e (eV)
		3.534±0.26 (Ref. 9)		1.06±0.22 (Ref. 3)
Experimental	$^7\Delta_u$ (Ref. 7)	3.817±0.036 (Ref. 8)	299.6 (Ref. 10)	0.78±0.17 (Ref. 4)
Theoretical *ab initio* calculations				
UHF (Ref. 4)	$^7\Sigma_u$	4.55	238.0	−1.74
CI (Ref. 4)	$^7\Delta_u$	4.54	204.0	−1.06
CI (Ref. 20)	$^7\Delta_u$	4.99	134.0	−1.71
$X\alpha$ (SW) (Ref. 23)	$^7\Delta_u$	3.78		
$X\alpha$ (SW) (Ref. 26)	$^7\Delta_u$	3.59±0.19		
LSD (Ref. 21)	$^7\Delta_u$	3.96	390	3.45
RHF (Ref. 19)	$^1\Sigma_g$	2.99	660	
Semiempirical calculations				
Extended Hückel (Ref. 17)	$^3\Sigma_g$	3.59 or 2.36		
Theoretical study of Mössbauer data				
UHF (Ref. 15)	$^3\Sigma_g$			
$X\alpha$ (DVM) (Ref. 22)	$^7\pi_u$			
$X\alpha$ (SW) (Ref. 23)	$^7\Sigma_g$ or $9\Sigma g$	3.97 or 4.16		3.1 or 5.0
Extended Hückel (Ref. 18)		7.52		

ic distance of 3.97 and 4.16 a.u., respectively.

Rohlfing *et al.*[26] performed $X\alpha$SW molecular-orbital calculations similar to that of Nagarathna *et al.*[23] with 10% overlapping spheres. The value of α chosen is not specified nor is the binding energy. They found an equilibrium bond length of 3.59 a.u. and the lowest-lying state is $^7\Delta_u$ for the Fe_2 ground state.

Our present work was motivated by the desire to develop an accurate method for the calculation of energies and wave functions of small transition-metal clusters in the local-spin-density approximation, without invoking any further approximation of the muffin-tin type, frozen core, etc., and without the use of any *ad hoc* parameter. Such an approach would definitely establish the proper spin states of the transition-metal diatomic molecules under the LSD approximation.

In this work a Gaussian orbital basis is employed and all relevant one-center and two-center, two-electron integrals are evaluated analytically. To accomplish this, we modified the standard quantum chemistry program GAUSSIAN82.

A special problem is encountered in regard to the exchange-correlation potential in this method. Although the charge densities are exactly expressed in terms of sums of Gaussian orbitals, the exchange-correlation potential is not. Rather than introducing an auxilliary fitting of the exchange-correlation potential using Gaussian orbitals, we have chosen to calculate the matrix elements of the potential by direct numerical integration on a semianalytical grid which takes advantage of the symmetry of the molecule. The grid is briefly described in the Appendix.

We describe our method in Sec. II, while the results of our computations are presented in Sec. III, which also contains a discussion and comparison of the results with experimental and with other calculations. The grid used for numerical integrations is described in the Appendix.

II. METHOD

According to the local-density-functional theory, the effective one-electron Hamiltonian for an electron of spin σ can be written as

$$H^\sigma = -\tfrac{1}{2}\nabla^2 + \sum_\mu \frac{Z_\mu}{|r-R_\mu|} + \int \frac{\rho(r')}{|r-r'|} d^3r' + V_{\rm xc}^\sigma(r) \ . \tag{2.1}$$

Atomic units, with energies in hartrees are used. In Eq. (2.1), $\rho(r)$ is the total charge density at the point r, R_μ is the position vector of the μth atom, and Z_μ is the atomic number of the atom. The quantity $V_{\rm xc}^\sigma(r)$ is the exchange-correlation potential for electrons of spin σ. Here we take this to be the parametrized exchange-correlation potential as given by Rajagopal, Singhal, and Kimball (RSK),[27] which has the von Barth–Hedin[28] functional form

$$V_{\rm xc}^\sigma = A(\rho)\left[\frac{2\rho^\sigma}{\rho}\right]^{1/3} + B(\rho) \ , \tag{2.2}$$

in which ρ^σ is the spin density and $A(\rho)$,$B(\rho)$ are numerical functions of density.

The functions $A(\rho)$ and $B(\rho)$ given in Ref. 28 depend on four filling parameters C^P, C^F, r^p, and r^f. For the RSK potential, $C^P=0.046\,12$, $C^F=0.026\,28$, $r^p=39.7$, $r^f=70.6$. The eigenfunctions Ψ_i^σ of H^σ are expanded in terms of a set of Gaussian basis functions ϕ_j, i.e.,

$$\Psi_i^\sigma = \sum_j C_{ij}^\sigma \phi_j \ . \tag{2.3}$$

The ϕ_j are, in general, not orthogonal. This leads to the secular equation

$$H^\sigma C^\sigma = E^\sigma S C^\sigma \ . \tag{2.4}$$

Here, H^σ denotes the Hamiltonian matrix for spin σ and S denotes the overlap matrix for the basis chosen. The electron-electron Coulomb interaction terms entail matrix elements of the form

$$\langle \phi_i(1)\phi(2) \,|\, 1/r_{12} \,|\, \phi_k(1)\phi_1(2)\rangle \ . \tag{2.5}$$

These matrix elements are evaluated exactly by using the two-electron integral routines of GAUSSIAN82. The matrix elements of the exchange-correlation potential are computed numerically on a two-dimensional grid using prolate spheroidal coordinates (see the Appendix).

Since H depends on C and σ, a self-consistent solution has to be found by an iterative process including two matrix diagonalizations (one for each value of σ) at each stage. The total energy is calculated from

$$E_t = \sum n_i^\sigma \varepsilon_i^\sigma - \tfrac{1}{2}\int\int \frac{\rho(r)\rho(r')}{|r-r'|} d^3r\, d^3r' + \Delta_{\rm xc} + \tfrac{1}{2}\sum_{\mu,\nu}{}' \frac{Z_\mu Z_\nu}{|r_\mu - R_\nu|} \ , \tag{2.6}$$

where $\Delta_{\rm xc}$ is given by

$$\Delta_{\rm xc} = E_{\rm xc} - \sum_\sigma \int \rho^\sigma(r) V_{\rm xc}^\sigma(r) d^3r \ , \tag{2.7}$$

and $E_{\rm xc}$ is the exchange-correlation function.

The binding energy is taken as the difference between the total energy of the molecule and the sum of the atomic energies of the two atoms, calculated in exactly the same manner as that of the molecule using the same numerical grid.

The vibrational frequency is found by fitting the potential-energy curve to a Morse potential,

$$E - E_m = D_e(1 - e^{-\beta(r-r_e)})^2 \ ,$$

in which r_e is the equilibrium internuclear distance, E_m is the minimum energy, D_e is the binding energy, and β is a parameter related to the vibrational frequency.

We perform a least-squares fit using

$$\ln\left[1 \pm \left[\frac{|E-Em|}{D_e}\right]^{1/2}\right] = -\beta(r-r_e)$$

to determine β, from which we find the vibrational frequency ω, as described by Herzberg.[29]

The basis sets used in this calculation consisted of Gaussian-type functions. For iron we have used the basis

set optimized for the atomic ground terms by Wachters.[16] This basis consists of 14s, 9p, and 5d uncontracted functions. The basis was improved by supplementing it with five s functions of exponents 657 539.0, 357 539.0, 0.041 889, 0.0093, and 0.007 889; two p functions of exponents 0.96 and 0.0751; four d functions of exponents 90.3545, 0.2015, 0.023 27, and 0.052 51; and an f function of exponent 0.5.

Since the iterative calculations leading to self-consistency were slow to converge, we defined a mixing factor λ such that the input density to the $(n+1)$th iterative stage is given by

$$\rho_{n+1}=\lambda\rho_n+(1-\lambda)\rho_{n-1}\ .$$

The value of λ chosen was always less than 0.1 in order to avoid oscillatory divergence of the procedure. As a result, a large number of iterations were necessary before the density matrix converged to the desired accuracy of 10^{-7}; λ is set equal to 1 towards the end of the iteration process to ensure that the proper converged state is obtained.

III. RESULTS AND DISCUSSION

In this section we present our results and compare them with experimental results and those of other calculations. We have studied the different spin states of the Fe_2 molecule and our calculations indicate that a $^7\Delta_u$ state with configuration

$$(6\sigma_{g\uparrow}^1 3\pi_{u\uparrow}^2 1\delta_{g\uparrow}^2 5\sigma_{u\uparrow}^1 1\delta_{u\uparrow}^2 6\sigma_{g\downarrow}^1 3\pi_{u\downarrow}^2 3\pi_{g\uparrow}^2 7\sigma_{g\downarrow}^1 6\sigma_{u\uparrow}^1 1\delta_{g\downarrow}^1)$$

and a $^9\Sigma_g$ state with configuration

$$(6\sigma_{g\uparrow}^1 1\delta_{g\uparrow}^1 3\pi_{u\uparrow}^2 1\delta_{u\uparrow}^2 3\pi_{g\uparrow}^2 7\sigma_{g\uparrow}^1 6\sigma_{g\downarrow}^1 6\sigma_{u\uparrow}^1 3\pi_{u\downarrow}^2 7\sigma_{g\downarrow}^1 7\sigma_{u\uparrow}^1)$$

are the two lowest-lying states of which $^7\Delta_u$ is the ground state lying about 0.56 eV below the $^9\Sigma_g$ state. The total energy of the iron atom ($3d^64s^2$) and the minimum total energy of the Fe_2 molecule in $^7\Delta$ and $^9\Sigma$ states are given in Table II.

Table III contains our results for the equilibrium separation, binding energy, and the vibrational frequency for the Fe_2 molecule in $^7\Delta_u$ and $^9\Sigma_g$ states. Figure 1 gives the potential-energy curves for the Fe_2 molecule for the above-mentioned spin states. It is clear that in the LSD approximation both $^7\Delta_u$ and $^9\Sigma_g$ are bound states and $^7\Delta_u$ is the ground state. The equilibrium separation of the ground state is 0.27 a.u. smaller than the equilibrium interatomic separation of the $^9\Sigma_g$ state. Figure 2 gives the low-lying energy levels of the molecule in the two spin states and these are compared to that of Ref. 26 for the $^7\Delta_u$ state and to that of Ref. 22 for the $^9\Sigma_g$ state. It can be seen that all the levels obtained in these calculations are lower than those of Refs. 26 and 22. This difference between the present result and those of Refs. 26 and 22 must be attributed to a combination of effects: different basis size and improvements introduced in the method of calculation which are primarily due to the introduction of correlation in the present work.

TABLE II. Minimum energies in the LSD approximation with RSK potential.

System	Total energy (hartrees)
Fe ($3d^64s^2$)	−1261.596 21
Fe_2 ($^7\Delta_u$)	−2523.298 62
Fe_2 ($^9\Sigma_g$)	−2523.269 96

Purdum *et al.*[8] used rare-gas matrix isolation techniques in combination with extended x-ray absorption fine structure (EXAFS) to study the interatomic distance of the Fe_2 molecule in solid neon. They observed that the interatomic distance of Fe_2 increased as the iron atomic percent concentration was increased. An Fe–Fe distance of 3.82 a.u.±0.038 for a concentration of 0.4 at. % of Fe was observed. Montano and Shenoy[9] performed a similar EXAFS experiment in the argon matrix. According to them, the Fe–Fe distance is 3.534±0.25 a.u. for a concentration of 0.1 at. % of Fe in Ar. At such concentrations they argue that there are mostly monomers and dimers present.

The interatomic distance of Fe_2 determined in the CI calculations[4,20] are close to the Fe–Fe distance in iron metal. The interatomic distance with the smaller basis is 0.15 a.u. smaller, and the one with the bigger basis is 0.32 a.u. larger, than the atomic separation of 4.687 a.u. in iron metal.

The LSD calculation of Harris and Jones[21] overestimates the Fe–Fe distance compared to the experimental results of Refs. 8 and 9 by 0.14 and 0.43 a.u., respectively.

The Fe–Fe distance of 3.59 a.u. reported by Rohlfing *et al.*[26] in the $X\alpha$ calculations is in good agreement with the experimental result of Ref. 9 and the Fe–Fe distance of 3.7 a.u. determined in this work is also in good agreement with all experimental data. It is very difficult to make an assessment at to which of the calculations gives the more accurate value of the equilibrium separation in Fe_2, because the experimental separation for a free Fe_2 molecule is not definitively known. However, the present value of 3.7 a.u. has been obtained from an all-electron calculation in which both electron exchange and correlation effects are taken into account and no approximation of the muffin-tin type has been involved, and we would

TABLE III. Ground-state properties of the Fe_2 molecule.

State	Equilibrium bond length r_e (a.u.)	Binding energy D_e (eV)	Vibrational frequency ω (cm^{-1})
Fe_2 ($^7\Delta_u$)	3.70±0.005	2.89	412±3
Fe_2 ($^9\Sigma_g$)	3.92±0.005	2.11	330±5

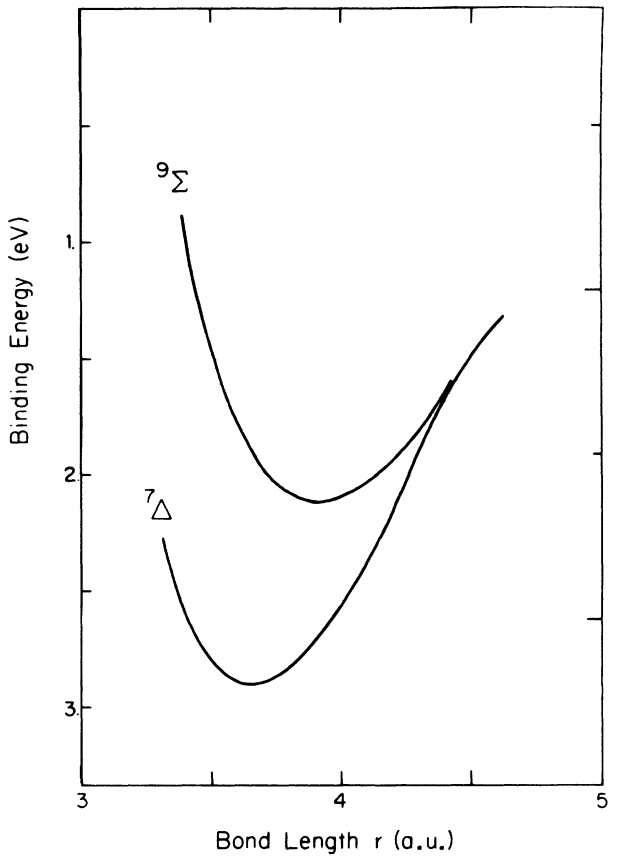

FIG. 1. Potential-energy curves as a function of internuclear separation for the $^9\Sigma_g$ and the $^7\Delta_u$ states of the Fe_2 molecule with RSK potential.

expect it to be more accurate.

As far as the vibrational frequency ω of the Fe_2 molecule is concerned, Moskovits and DiLella[10] determined the frequency to be 299 cm^{-1} from the resonance Raman spectra of $^{56}Fe_2$ isolated in solid Ar and Kr. The previous theoretical value in LSD approximation is that of Harris and Jones,[21] which is 91 cm^{-1} (30%) larger than the experimental values. The present calculation reports a vibrational frequency of 412 cm^{-1}, which is 22 cm^{-1} higher than that of Harris and Jones. The CI values of 134 and 204 cm^{-1} with large and small basis sets underestimate the vibrational frequency by 55% and 32%, respectively. The value of 600 cm^{-1} derived from RHF calculations is incompatible with all other values. However, the value of ω determined in this work for the $^9\Sigma_g$ state is 330 cm^{-1}, which is only 13% larger than the experimental value. Similarly, the equilibrium distance and the binding energy of the $^9\Sigma_g$ state are in good agreement with quoted experimental data. Energetically, in the LSD approximation, $^7\Delta_u$ is definitely the ground state. However, the symmetry of the Fe_2 molecule formed by the matrix isolation technique is not definitely established, and could differ from the free dimer-state and from the minimum-energy state found here.

Lin and Kant[3] estimated to dissociation energy D_e of the Fe_2 molecule using high-temperature mass-spectrometric techniques. The third-law dissociation energy of 1.04±0.22 eV was estimated by them. This determination of the dissociation energy was based on calculations in which the interatomic separation of Fe_2 molecule was assumed to be 4.403 a.u. and the vibrational frequen-

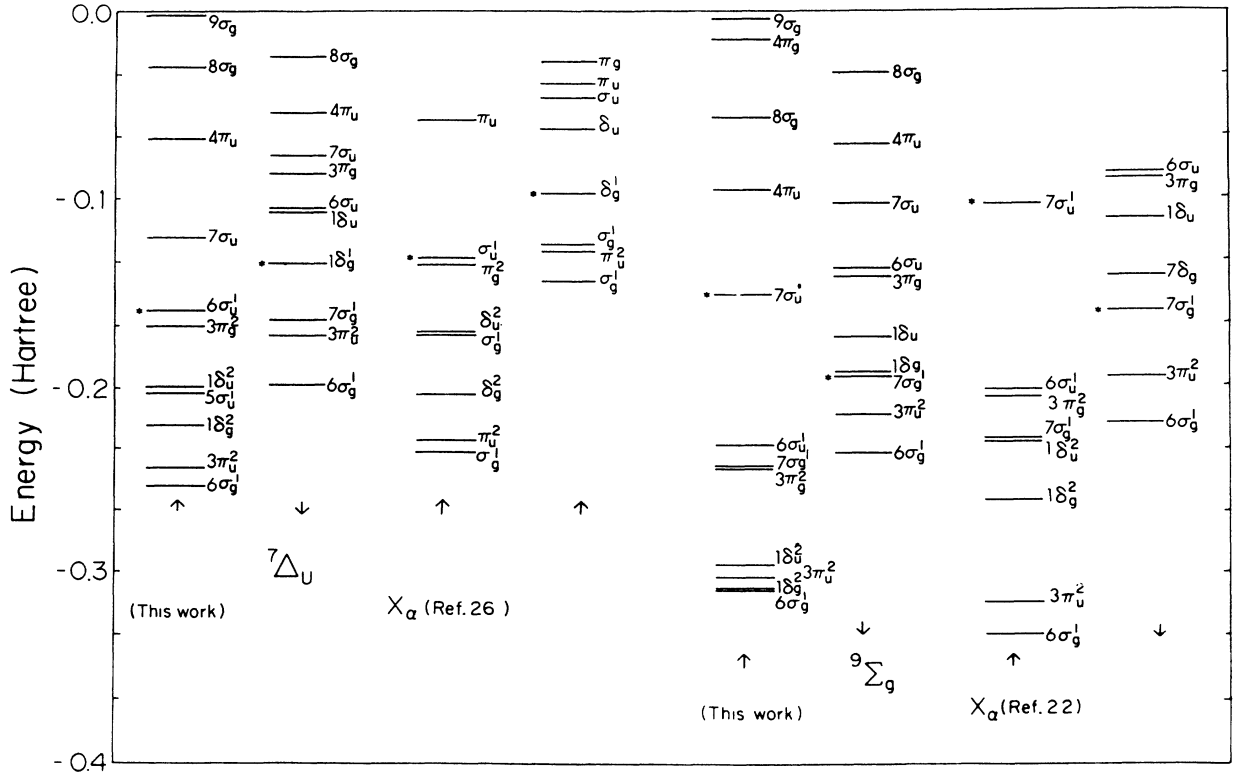

FIG. 2. Orbital energy levels for the iron dimer at the equilibrium interatomic distances for the $^7\Delta_u$ and the $^9\Sigma_g$ states (* indicates the highest occupied level).

cy 365 cm^{-1}. As mentioned earlier, the vibrational frequency is not known and the equilibrium separation of Fe_2 is definitely lower than 4.4 a.u. This raises a serious question about the accuracy of the analysis which led to the value of the dissociation energy of Fe_2.

In the HF calculations and the only CI calculation, the Fe_2 molecule is not bound. In the LSD approximation, only Harris and Jones[21] have determined the binding energy. Their value of 3.45 eV is very much larger than the experimental value of 1.04 eV and also larger than the 2.89 eV obtained in our calculations. It is known that the LSD approximation for most diatomic molecules overestimates binding, but the extent of overbinding in the present calculation cannot be determined as the experimental value is so uncertain. The difference between the present result and that of Harris and Jones must be attributed to a combination of effects.

(a) We have made a full spin-polarized calculation, whereas their calculation is not fully spin polarized.

(b) We have calculated all the one-center and two-center two-electron integrals analytically, whereas they employed a quasiatomic potential with muffin-tin spheres and some *ad hoc* adjustable parameters to calculate the matrix elements.

(c) We have used a large uncontracted basis, whereas the basis used by them is not mentioned. The basis size will also have some effects.

These differences do appear to be major and the results obtained here do differ fairly significantly from those of Harris and Jones, and in most of the instances examined, the difference is in the direction of improved agreement with the available experiment.

For the Fe_2 ($^7\Delta_u$) molecule we show in Fig. 3 (a) a three-dimensional plot of the net spin density on a plane through the internuclear axis of the molecule, and (b) the contour plot of the net spin density. There are regions of small minority spin excess perpendicular to the internuclear axis lying midway between the two nuclei, in the exterior of the molecule along the internuclear axis, and another small region very close to the nuclei. This can be clearly seen in Fig. 4(a) in which the net spin density along the axis of the molecule is plotted, and in Fig. 4(b) which shows the net spin density along a direction perpendicular to the molecular axis and passing through one of the nuclei. The spin density at the Fe nucleus has the value 0.110 22 a.u. and the total charge density at the nucleus is 11 662.8 a.u.

For the Fe_2 ($^7\Delta$) molecule we show in Fig. 5(a) a three-dimensional plot of the charge density for the $1\delta_{g\downarrow}$ orbital on a plane through the internuclear axis of the molecule and in Fig. 5(b) the contour plot of the same charge density. Figures 6–8 show similar three-dimensional and contour plots of the charge density for the $6\sigma_{\uparrow}$, $7\sigma_{g\downarrow}$, and

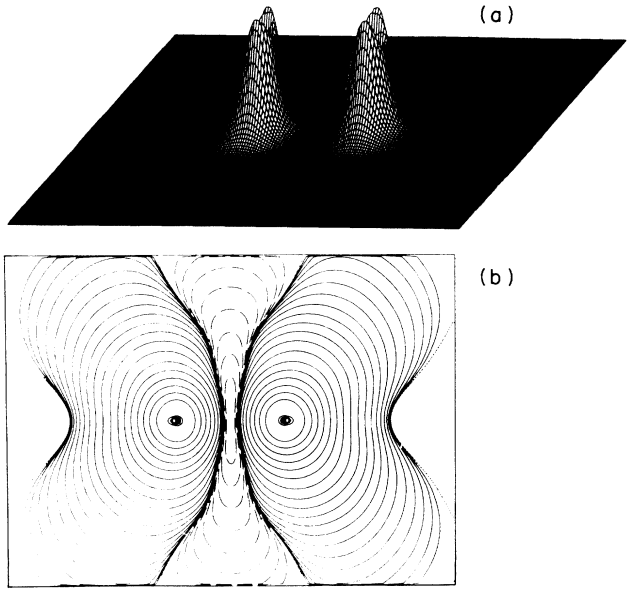

FIG. 3. (a) Three-dimensional plot of the net spin density of the Fe_2 ($^7\Delta_u$) molecule at the equilibrium interatomic distance on a plane passing through the molecular axis. (b) Contour plot of the net spin density of the Fe_2 ($^7\Delta_u$) molecule. Solid lines indicate majority spin predominancy, dashed lines minority spin. The majority spin contours correspond to spin density of $(0.8769/2^n)\,a_0^{-3}$ for the outermost contour $n=21$. The minority spin contours corresponds to spin density of $(-0.025\,67/2^n)a_0^{-3}$, for the innermost contour $n=10$.

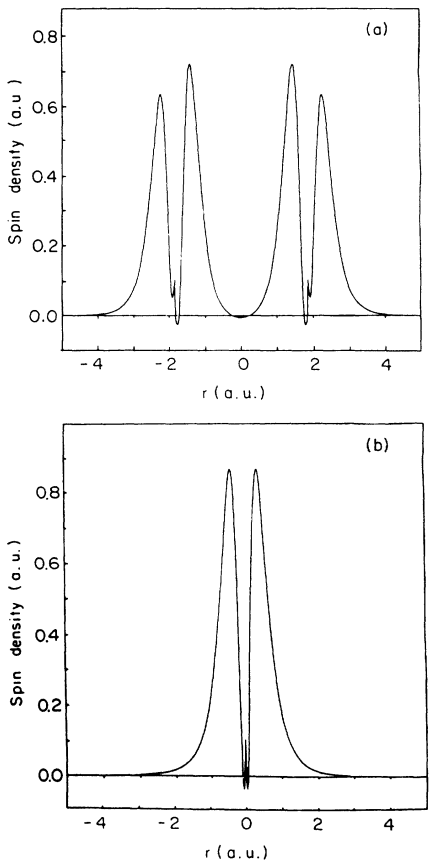

FIG. 4. (a) Net spin density along the molecular axis for Fe_2 in the $^7\Delta_u$ state. (b) Net spin density along a direction perpendicular to the molecular axis of Fe_2 ($^7\Delta_u$) and passing through one of the nuclei.

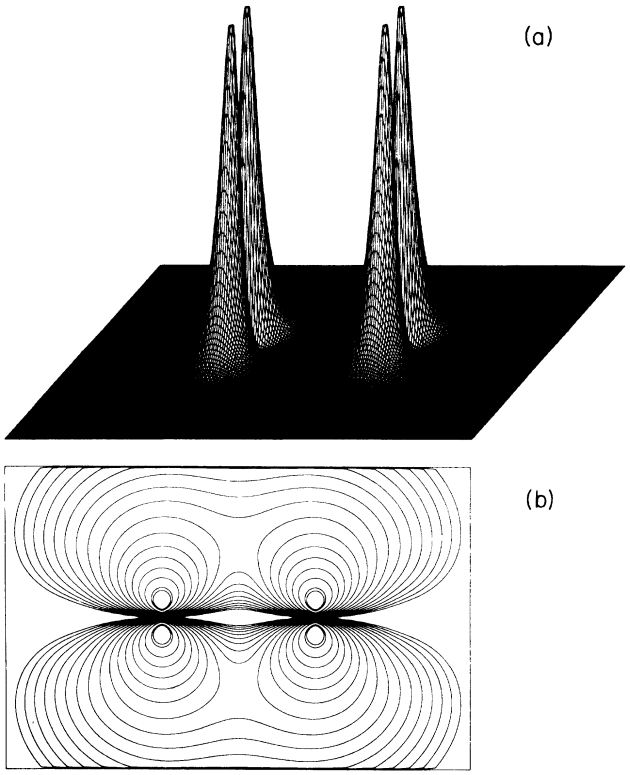

FIG. 5. (a) Three-dimensional plot of the charge density of the $1\delta_{g\downarrow}$ molecular orbital of Fe_2 ($^7\Delta_u$). (b) Contour plot of the same charge density as in (a). The contour corresponds to a charge density of $(0.1994/2^n)a_0^{-3}$ for the outermost contour $n=17$.

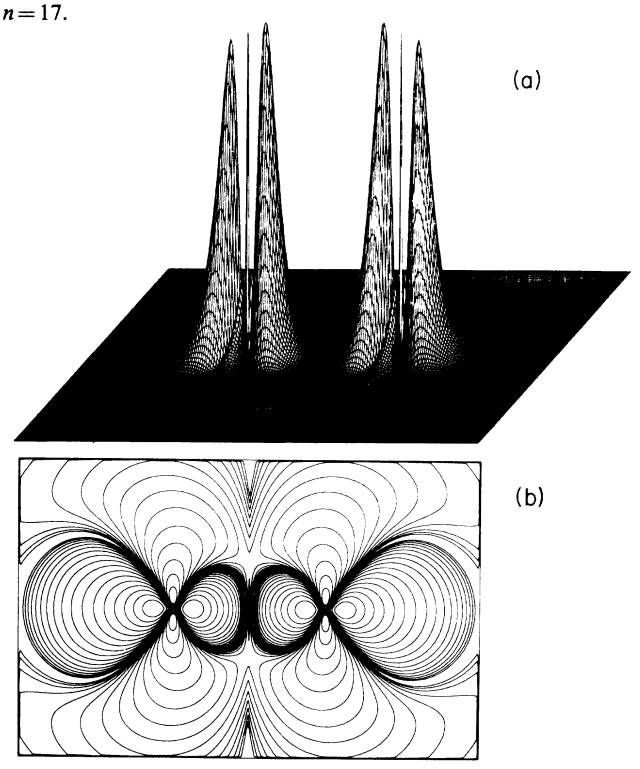

FIG. 6. (a) Three-dimensional plot of the charge density of the $6\sigma_{u\uparrow}$ molecular orbital of Fe_2 ($^7\Delta_u$). (b) Contour plot of the same charge density as in (a). The contour corresponds to a charge density of $(0.5865/2^n)a_0^{-3}$ for the outermost contour $n=21$.

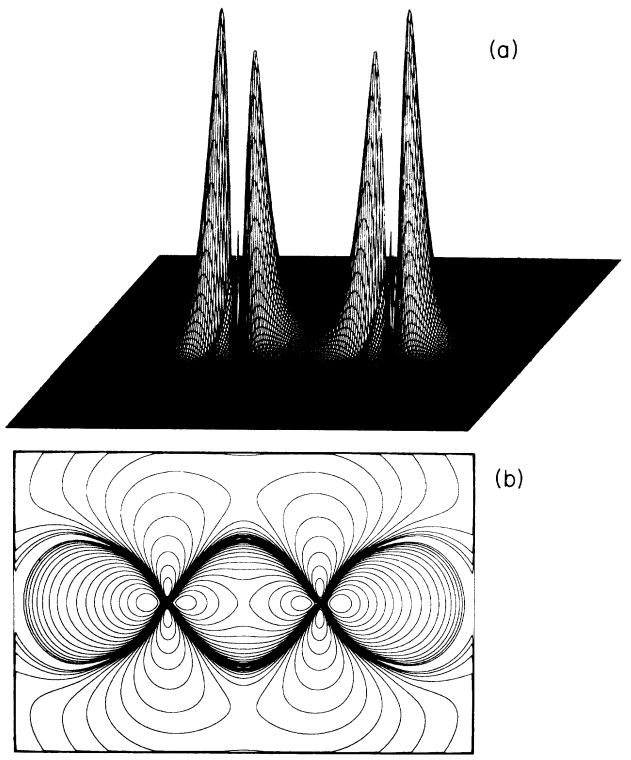

FIG. 7. (a) Three-dimensional plot of the charge density of the $7\sigma_{g\downarrow}$ molecular orbital of Fe_2 ($^7\Delta_u$). (b) Contour plot of the same charge density as in (a). The contour corresponds to a charge density of $(0.4536/2^n)a_0^{-3}$ for the outermost contour $n=21$.

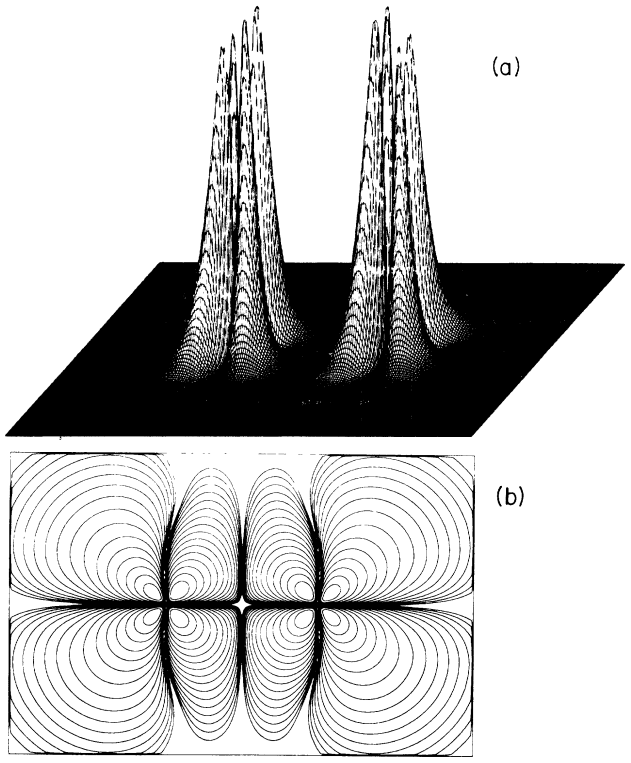

FIG. 8. (a) Three-dimensional plot of the charge density of the $3\pi_{u\uparrow}$ molecular orbital of Fe_2 ($^7\Delta_u$). (b) Contour plot of the same charge density as in (a). The contour corresponds to a charge density of $(0.2576/2^n)a_0^{-3}$ for the outermost contour $n=17$.

$3\pi_{u\uparrow}$ orbitals of the molecule, respectively.

It can be seen from these plots that the $1\delta_{g\downarrow}$ orbital of the minority spin at the Fermi level and the $6\sigma_{g\downarrow}$ orbital are mainly responsible for bonding in the molecule, while the majority spin $6\sigma_{u\uparrow}$ and $3\pi_{g\uparrow}$ orbitals close to the Fermi level do not contribute to binding.

It is difficult to be quantitatively precise concerning the accuracy of the present results. Other authors have not given the total energies as calculated in the local-spin-density approximation. We have chosen to do so in the hope of assisting others in the evaluation of our results. It is our belief concerning the internal mechanics of the calculation, which includes matrix diagonalization, word length, etc., that the quoted total energies are accurate to the number of figures stated. More uncertain are the basis-set size effects and accuracy of numerical integration on the grid.

The virial ratio (the ratio of potential energy to kinetic energy) at the equilibrium separation is 2.001. The error in the virial ratio is only 0.05% from the exact value. For this complicated system the basis set is larger in size than that used in the best studies of transition-metal dimers.

To test the precision of the numerical grid used for calculating the matrix elements of the exchange-correlation potential we used the value of $N=\int \rho(r)d^3r$ as a test of accuracy. For each value of the interatomic distance, we adjusted the grid size so that there was no difference between the calculated and the exact value of N up to seven significant figures. This also gave the minimum total energy at the particular interatomic separation. Such accuracy required a grid of 1152 points in one-quarter of the plane.

The total energy of the isolated atoms was obtained with the same basis on the same numerical grid as was used for molecular calculations. The energy of the atom so obtained is within 0.0006 hartrees of the exact nonvariational total energy obtained by direct numerical integration of the effective Schrödinger equation, as described in Refs. 30 and 31. Therefore we believe that the basis set used is close to complete and our result is very close to convergence. Additional improvements in the basis sets or the grid sizes would not change our conclusions concerning the electronic structure and the spectroscopic constants of the Fe_2 molecule reported in this article.

ACKNOWLEDGMENTS

The authors wish to thank Professor Joseph Callaway of Louisiana State University and Dr. G. S. Painter of Oak Ridge National Laboratory for helpful and interesting discussions. This work was supported by U.S. Department of Energy Grant No. DE-FG05-87ER13674 from the Division of Chemical Sciences, Office of Basic Energy Sciences.

APPENDIX

Prolate spheroidal coordinates have been chosen for generating the two-dimensional mesh on which the matrix elements of the exchange-correlation potential V_{xc}^{σ} are evaluated. These coordinates are discussed in most of the mathematical physics textbooks and also by Wahl, Cade, and Roothaan.[32] Assuming that the confocal ellipsoids and hyperboloids of revolution have the foci located at Cartesian coordinates (0,0,a) and (0,0,b), then the coordinate (x,y,z) of any point can be written in prolate spherical coordinates as

$$\begin{aligned} x &= R\,\sinh u\,\sin v\,\cos\phi\ , \\ y &= R\,\sinh u\,\sin v\,\sin\phi\ , \\ z &= R\,\cosh u\,\cos v\ , \end{aligned} \tag{A1}$$

where u and v define the ellipsoid and hyperboloid surfaces, respectively, ϕ is the azimuthal angle, and R is the separation of the two foci ($R=|a-b|$). The domains of U, v, and ϕ are $0\le U<\infty$; $0\le U\le\pi$ and $0\le\phi\le 2<2\pi$.

If we denote by r_a and r_b the distances of a point (x,y,z) from the two foci, then the prolate spherical coordinates can also be defined by

$$\begin{aligned} \xi &= (r_a+r_b)/R=\cosh u\ , \\ \eta &= (r_a-r_b)/R=\cos v\ , \\ \phi &= \phi\ , \end{aligned} \tag{A2}$$

and the domains of ξ, η, and ϕ are $1\le\xi<\infty$, $-1\le\eta\le 1$, and $0\le\phi\le 2\pi$. In this form, the Cartesian coordinates (x,y,z) can then be written as

$$\begin{aligned} x &= \frac{R}{2}(\xi+\eta)\left[1-\frac{1+\xi\eta}{\xi+\eta}\right]^{1/2}\cos\phi\ , \\ y &= \frac{R}{2}(\xi+\eta)\left[1-\frac{1+\xi\eta}{\xi+\eta}\right]^{1/2}\sin\phi\ , \\ z &= \frac{R}{2}(\xi+\eta)\left[1+\frac{\xi\eta}{\xi+\eta}\right]+R\ , \end{aligned} \tag{A3}$$

and the element of volume

$$\begin{aligned} dV &= dx\,dy\,dz \\ &= (R/2)(\xi^2-\eta^2)d\xi\,d\eta\,d\phi\ . \end{aligned} \tag{A4}$$

The semi-infinite domain of ξ is transformed into a finite domain ($1\le\xi\le\xi_{max}$) by the transformation

$$\xi=\frac{1+\beta}{1-\beta\eta}\ . \tag{A5}$$

The parameter $\beta(0<\beta<1)$ is adjusted so the values of $V_{xc}^{\sigma}(r_{max})$ and $\rho(r_{max})$ are negligible. Thus β defines ξ_{max}, which specifies the prolate spheroidal region of integration, i.e.,

$$\xi_{max}=\frac{1+\beta}{1-\beta}\ . \tag{A6}$$

The values of η and $d\eta$ are taken as the roots and the weight factors of a Gauss-Legendre quadrature, respectively. If the value of β is fixed we get a set of well-defined points of integration $r_i(x_i,y_i,z_i)$ and the corresponding weight factors $w(r_i)(=dv)$ from Eqs. (A3) and

(A4), respectively.

The spin density required to calculate V_{xc}^{σ} is computed at each grid point from the eigenfunctions Ψ_k^{σ} and the occupation numbers n_k^{σ},

$$\rho^{\sigma}(r)=\sum_{i,j}\sum_{k} n_i^{\sigma}\phi(r)\phi(r)C_{ik}C_{jk}$$
$$=\sum_{i,j} D_{ij}^{\sigma}\phi_i(r)\phi_j(r) , \quad \text{(A7)}$$

where $D_{ij}^{\sigma}=\sum_k n_i^{\sigma}C_{ik}C_{jk}$, the σ spin-density matrix.

The matrix elements of V_{xc}^{σ} are given by

$$\langle \phi_k \mid V_{xc}^{\sigma} \mid \phi_j \rangle = \sum_{i=1} \phi(r_i)\phi_j(r_i)W(r_i)G_{kj} , \quad \text{(A8)}$$

in which the sum runs over all grid points r_i, $W(r_i)$ is a weight associated with the grid point, and G_{kj} is given by

$$G_{kj}=\int_0^{2\pi}\Omega_k(\phi)\Omega_j(\phi)d\phi , \quad \text{(A9)}$$

where $\Omega_j(\phi)$ is the function giving the azimuthal dependence of ϕ_j [for an s function, $\Omega(\phi)=1$; for a p function, $\Omega_{p_x}(\phi)=\sin\phi$, $\Omega_{p_y}(\phi)=\cos\phi$, $\Omega_{p_z}(\phi)=1$, etc.]. G_{kj} is computed analytically.

[1]K. A. Gingerich, J. Cryst. Growth **9**, 31 (1971).
[2]K. A. Gingerich, Cum. Top. Met. Sci. **6**, 345 (1980).
[3]S. S. Lin and A. Kant, J. Phys. Chem. **73**, 2450 (1969).
[4]I. Shim and K. A. Gingerich, J. Chem. Phys. **77**, 2490 (1982).
[5]A. Kant, S. S. Lin, and B. Strauss, J. Chem. Phys. **49**, 1983 (1968).
[6]G. Vewrhaegen, S. Smoes, and J. Drowart, J. Chem. Phys. **40**, 239 (1964).
[7]D. M. Cox, D. J. Trevor, R. L. Whetten, E. A. Rohlfing, and A. Kaldor, Phys. Rev. B **32**, 7290 (1985).
[8]H. Purdum, P. A. Montano, G. K. Shenoy, and T. Morrison, Phys. Rev. B **25**, 4412 (1982).
[9]P. A. Montano and G. K. Shenoy, Solid State Commun. **35**, 53 (1980).
[10]M. Moskovits and D. P. DiLella, J. Chem. Phys. **73**, 4917 (1980).
[11]M. Moskovits, D. P. DiLella, and W. Limm, J. Chem. Phys. **80**, 626 (1984).
[12]V. E. Bondybey and J. H. English, Chem. Phys. Lett. **94**, 443 (1983).
[13]K. P. Huber and G. Herzberg, *Molecular Spectra and Molecular Structure IV* (Van Nostrand Reinhold, New York, 1979).
[14]M. D. Morse, G. P. Hansen, P. R. R. Langridge-Smith, L.-S. Zheng, M. E. Geusic, D. L. Micholopoulos, and R. E. Smalley, J. Chem. Phys. **80**, 5400 (1984).
[15]P. C. Kelires, K. C. Mishra, K. J. Duff, and T. P. Das, Phys. Rev. B **34**, 4529 (1986).
[16]A. J. H. Wachters, J. Chem. Phys. **52**, 1033 (1970).
[17]W. F. Cooper, G. A. Clark, and C. R. Hare, J. Phys. Chem. **76**, 2268 (1972).
[18]A. Trautwein and Frank E. Harris, Phys. Rev. B **7**, 4755 (1973).
[19]A. Wolf and H.-H. Schmidtke, Int. J. Quantum Chem. **18**, 1187 (1980).
[20]*Ten Papers in the Exact Sciences and Geology. Part One of Sixteen Research Reports,* edited by J. Lindhard (Kongelige Danske Videnskabernes Selskab Matematisk-fysiske, Copenhagen, 1985).
[21]J. Harris and R. O. Jones, J. Chem. Phys. **70**, 830 (1979).
[22]D. Gvenzburger and E. M. B. Saitovitch, Phys. Rev. B **24**, 2368 (1981).
[23]H. M. Nagarathna, P. A. Montano, and V. M. Naik, J. Am. Chem. Soc. **105**, 2938 (1983).
[24]K. Schwarz, Phys. Rev. B **5**, 2466 (1972).
[25]J. G. Norman, J. Chem. Phys. **61**, 4630 (1974).
[26]E. A. Rohlfing, D. M. Cox, A. Kaldor, and K. H. Johnson, J. Chem. Phys. **81**, 3846 (1984).
[27]A. K. Rajagopal, S. P. Singhal, and J. Kimball (unpublished); cited by A. K. Rajagopal in *Advances in Chemical Physics,* edited by G. I. Prigogine and S. A. Rice (Wiley, New York, 1979), Vol. 41, p. 59.
[28]U. von Barth and L. Hedin, J. Phys. C **5**, 1629 (1972).
[29]G. Herzberg, *Molecular Spectra and Molecular Structure* (Van Nostrand, New York, 1950), p. 401.
[30]S. Dhar and J. Callaway, Phys. Rev. A **35**, 4475 (1987).
[31]V. L. Moruzzi, J. F. Janak, and A. R. Williams, *Calculated Electronic Properties of Metals* (Pergamon, New York, 1978).
[32]A. C. Wahl, P. E. Cade, and C. C. J. Roothaan, J. Chem. Phys. **41**, 2578 (1964).

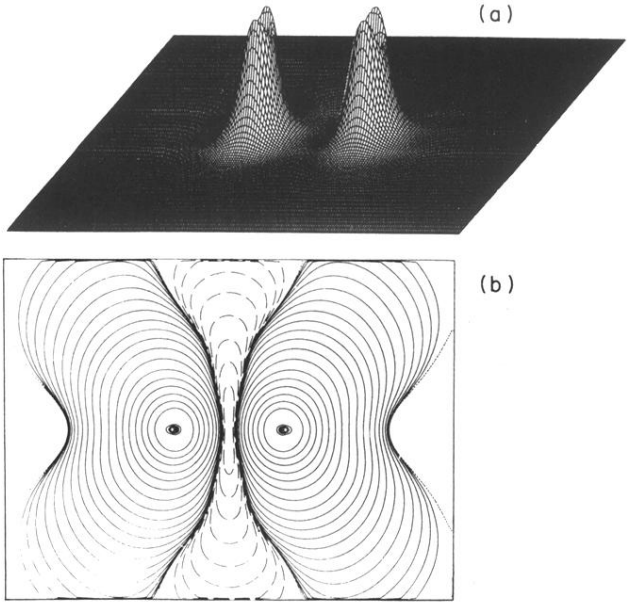

FIG. 3. (a) Three-dimensional plot of the net spin density of the Fe_2 ($^7\Delta_u$) molecule at the equilibrium interatomic distance on a plane passing through the molecular axis. (b) Contour plot of the net spin density of the Fe_2 ($^7\Delta_u$) molecule. Solid lines indicate majority spin predominancy, dashed lines minority spin. The majority spin contours correspond to spin density of $(0.8769/2^n)\, a_0^{-3}$ for the outermost contour $n=21$. The minority spin contours corresponds to spin density of $(-0.025\,67/2^n)a_0^{-3}$, for the innermost contour $n=10$.

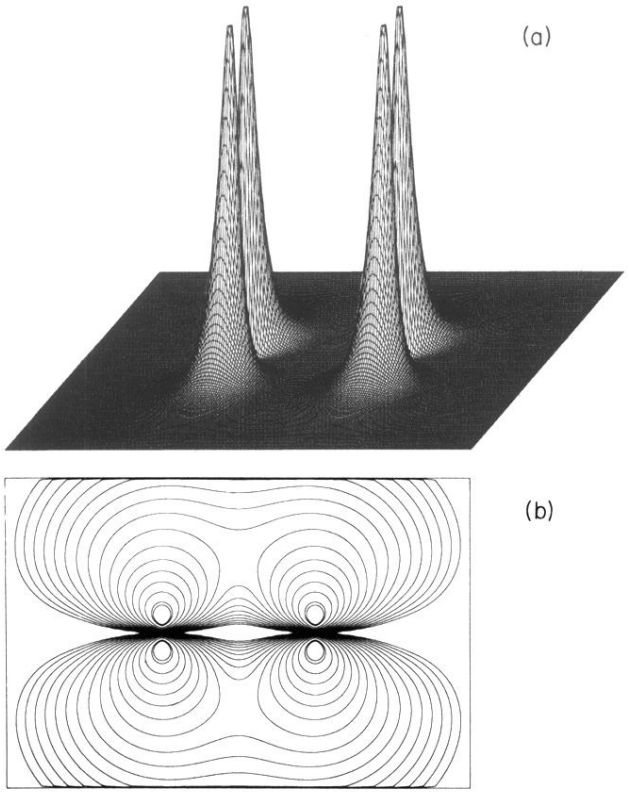

FIG. 5. (a) Three-dimensional plot of the charge density of the $1\delta_{g\downarrow}$ molecular orbital of Fe_2 ($^7\Delta_u$). (b) Contour plot of the same charge density as in (a). The contour corresponds to a charge density of $(0.1994/2^n)a_0^{-3}$ for the outermost contour $n=17$.

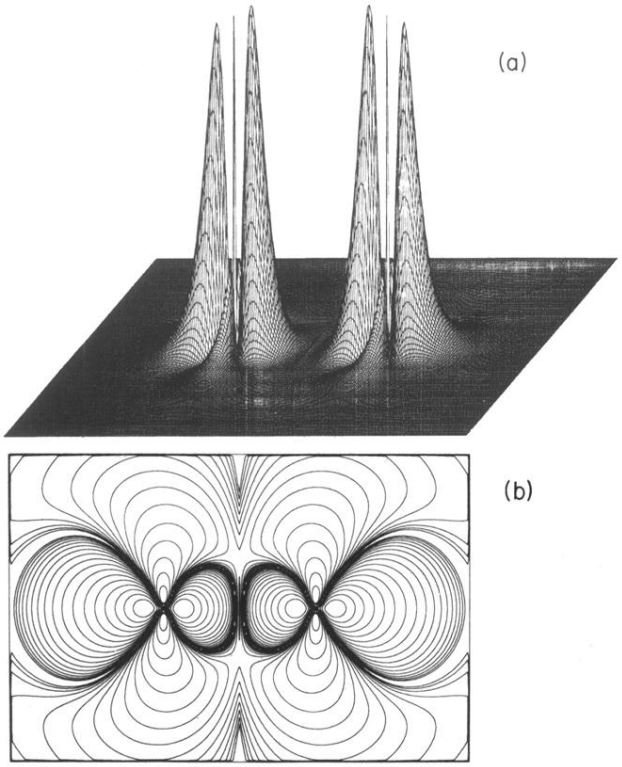

FIG. 6. (a) Three-dimensional plot of the charge density of the $6\sigma_{u\uparrow}$ molecular orbital of Fe_2 ($^7\Delta_u$). (b) Contour plot of the same charge density as in (a). The contour corresponds to a charge density of $(0.5865/2^n)a_0^{-3}$ for the outermost contour $n=21$.

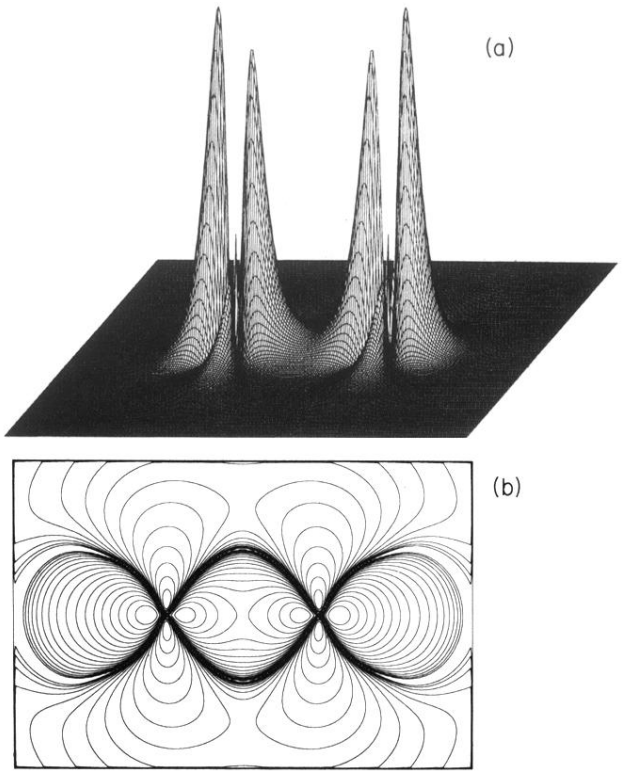

FIG. 7. (a) Three-dimensional plot of the charge density of the $7\sigma_{g\downarrow}$ molecular orbital of Fe_2 ($^7\Delta_u$). (b) Contour plot of the same charge density as in (a). The contour corresponds to a charge density of $(0.4536/2^n)a_0^{-3}$ for the outermost contour $n=21$.

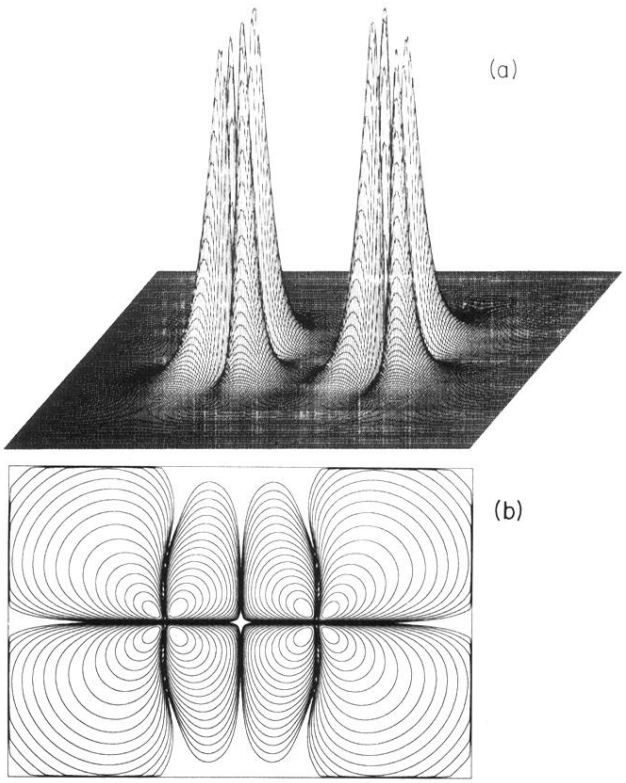

FIG. 8. (a) Three-dimensional plot of the charge density of the $3\pi_{u\uparrow}$ molecular orbital of Fe_2 ($^7\Delta_u$). (b) Contour plot of the same charge density as in (a). The contour corresponds to a charge density of $(0.2576/2^n)a_0^{-3}$ for the outermost contour $n=17$.